At Shell Polymers, we're dedicated to helping our customers create a stronger polyethylene supply chain. That's why we're reimagining the polyethylene industry with our state-of-the-art plant technologies and trusted, tested industry experts. This commitment to offering an unrivaled customer experience by streamlining your supply chain is just one way we **Break the Mold.**

SHELL POLYMERS
MAKING THE EXPERIENCE MATTER

Click here to learn more about Shell Polymers

Received: 22 June 2020 | Revised: 10 July 2020 | Accepted: 11 July 2020

DOI: 10.1002/pol.20200435

ORIGINAL ARTICLE

JOURNAL OF POLYMER SCIENCE WILEY

Chain-growth polycondensation via the substituent effect: Investigation of the monomer structure on synthesis of poly(N-octyl-benzamide)

Frederick C. Prehn Jr[1] | **Brian D. Etz**[1] | **Caleb J. Reese**[2] | **Shubham Vyas**[1] | **Stephen G. Boyes**[2]

[1]Department of Chemistry, Colorado School of Mines, Golden, Colorado

[2]Department of Chemistry, The George Washington University, Washington, District of Columbia

Correspondence
Stephen G. Boyes, Department of Chemistry, The George Washington University, Washington, DC 20052.
Email: sboyes@gwu.edu

Funding information
National Science Foundation, Grant/Award Number: CHE MSN #1807863

Abstract

A systematic study of the behavior of different leaving groups on a variety of ester-based monomers was performed for the chain-growth polycondensation synthesis of poly(N-octyl benzamide). Linear and branched alkane esters were compared with their phenyl analogs using both computational and experimental methods. Kinetic experiments along with qualitative solubility observations were used, with the aid of nuclear magnetic resonance spectroscopy and gel-permeation chromatography, to determine progress of the reaction, molecular weights, and molecular weight distributions. It was found that the reactivity of the monomer's ester group depends more on the stability of the leaving alkoxide than the electrophilicity of the carbonyl carbon, which contradicts previous literature. The order of reactivity increases for the alkyl esters with decreasing steric hindrance and decreasing pKa of the substituent. For the phenyl ester derivatives, the more electron withdrawing character of a para substituent increases the reactivity of the ester group, due to the higher resonance stabilization of the leaving phenoxide anion, not due to an increase in the electrophilicity of the carbonyl carbon.

KEYWORDS

chain growth polycondensation, monomer design, polyamide, substituent effect

1 | INTRODUCTION

Polycondensation techniques have been utilized to create a wide variety of polymers that span many disciplines. Typically, polymers derived using polycondensation techniques utilize the conventional step-growth method, where functional groups on both sides of the monomers randomly react with one another to assemble the polymer in a "stepwise" fashion. This process typically produces relatively low molecular weight polymers with a reasonably broad molecular weight distribution (polydispersity index, PDI or M_w/M_n, approaching 2.0) as the reaction approaches high monomer conversions.[1] In addition, it is difficult to obtain accurate control over the molecular weight in step-growth polymerizations and they do not allow for the preparation of well-defined block copolymers. In an attempt to overcome these limitations and expand the use of polymers traditionally made via the step-growth process, new polymerization methods have developed to produce conventional step-growth polymers via a chain-growth mechanism, where the reactivity of the polymer end group can be favored over other reactions.[2–5]

The theory and practice behind converting step-growth to chain-growth condensation (CGC) via the substituent effect was pioneered by Yokozawa and

coworkers and has been extensively reviewed.[2,3,6–9] Utilization of the CGC processes provides control over properties by achieving planned molecular weights with defined chain end groups, along with producing polymers with a narrow molecular weight distribution. The CGC process, like other traditional living polymerization techniques, allows for the synthesis of block copolymers, and more recently, the synthesis of surface-initiated polymer brushes from polymers traditionally prepared using step-growth polymerization.[10,11]

Aromatic polyamides are selected by industry for their impressive mechanical and thermal properties and notable chemical resistance.[12] Conventionally, the most famous aromatic polyamides, such as Kevlar© and Nomex©, are synthesized using a step-growth process where an aromatic diamine is reacted with a corresponding aromatic diacid chloride, producing very robust materials, due to the strength and stability of the aromatic backbones and the presence of hydrogen bonding. Because of their excellent properties, aromatic polyamides are produced in high volumes every year. Aromatic polyamides have the potential for an even wider impact on materials science and engineering if they could be produced using a controlled polymerization technique, that would allow for the production of polymers with a predetermined molecular weights and narrow molecular weight distribution. Controlled polymers allow for potentially improved functionality and solubility, and the ability to create more complex architectures such as block copolymers or covalently attaching the polymers to surfaces to produce well-defined polymer films.

With this in mind, Yokozawa and coworkers have developed multiple synthesis schemes that produce living, CGC aromatic polyamides in solution.[3,13–17] While the majority of Yokozawa's work has focused on N-substituted aromatic polyamides, he has also demonstrated the ability to prepare conventional nonsubstituted aromatic polyamides, which are required to obtain the favorable properties discussed above. The mechanism responsible for the conversion from step-growth to chain-growth involves deactivating the monomer towards self-condensation, while activating an initiator, or the end group of the polymer, so monomer preferentially adds in a chain-growth manner.

Recently, our group addressed the challenge of producing aromatic polyamide brushes utilizing the CGC technique.[11] This was achieved by designing an activated CGC initiator that has the capability to attach to silica surfaces. After attachment of the initiator, it was demonstrated for the first time that aromatic polyamide brushes could be grown from these surfaces using this CGC technique. However, during this study it was observed that while the polymerization would occur as expected, only low molecular weight polymers would form from the surface, resulting in relatively low brush thicknesses, before the system appeared to self-terminate. In addition, it was also observed that during the polymerizations using monomers containing the methoxide leaving group, an insoluble by-product was produced during the polymerization. Analysis of this by-product determined it to be lithium methoxide aggregates, produced in solution as part of the polymerization mechanism. When conducting a surface-initiated polymerization, these aggregates produced a film on the silica wafer surface, which was hypothesized to block monomer from reaction with the end group of the polymers and, subsequently, inhibit further brush growth.

As a result of these observations, the following study has been conducted to investigate the factors that influence the overall CGC mechanism, kinetics, and by-product stability and solubility. While the effect of ester structure on nucleophilic acyl substitution has been widely studied, this knowledge has not been applied to provide a better understanding of the CGC mechanism. In fact, the proposed mechanism for the CGC polymerization reaction does not take into account the effect of the leaving group at all and focuses solely on the reactivity of the carbonyl group.[2,3,6–9] As such, it is important to understand and incorporate the effect of the ester monomer structure on the CGC mechanism to be able to optimize the system. To achieve this, the experiments focused on the nature of the ester leaving group and how this affects the polymerization performance and resulting solubility of the condensation products, along with how these affect the ability to achieve controlled molecular weights and narrow molecular weight distributions.

This study focuses on two different categories of ester monomers: alkyl esters (straight chain and branched), and phenyl derivatives with varying para-substituents (electron donating and electron withdrawing character). To assist in understanding the results obtained in this study, reaction energetics were obtained through theoretical calculations along with computation of partial atomic charges.

2 | EXPERIMENTAL

2.1 | Materials

Lithium 1,1,1,3,3,3-hexamethyldisilazide (LiHMDS, 1.0 M) in tetrahydrofuran (THF), dimethylamine solution (2 M, THF), triethylamine (>99.5%), thionyl chloride ($SOCl_2$, >99.5%), anhydrous dichloromethane (DCM) (stabilized with 50–150 ppm amylene, >99.8%), octanal (99%),

sodium triacetoxyborohydride (97%), and $MgSO_4$ were purchased from Sigma Aldrich. DCM, acetic acid, $NaHCO_3$, NaOH, and ethyl acetate were purchased from Macron. Ammonium chloride (99.9%) was purchased from Baker Scientific and methyl 4-aminobenzoate (98%) from Alfa Aesar. Unless otherwise mentioned, all chemicals were used as received without further purification. THF was purchased from Macron and was purified and dispensed through a PURE SOLV MD-4 solvent purification system (activated alumina, copper catalysts and molecular sieves).

2.2 | Instruments and characterization

^1H and ^{13}C nuclear magnetic resonance (NMR) spectra were obtained on a JEOL-500S MHz spectrometer. Infrared spectra were recorded on a Thermo Scientific Nicolet iS50 Fourier transform infrared (FTIR) spectrometer using a diamond attenuated total reflectance (ATR) crystal. Number-average molecular weight (M_n) and polydispersity index (M_w/M_n, PDI) were measured using a Viscotek GPCmax gel-permeation chromatography (GPC) unit (eluent: stabilized THF (OmniSolv) with a flow rate of 1.0 ml/min using PLgel 5 μm MIXED-C and MIXED-D columns: molecular weight range 200–2,000,000 and 200–400,00 g/mol (polystyrene equivalent), respectively). A d*n*/d*c* value for the prepared polymers of 0.156 was determined and used during the analysis.

2.3 | Synthesis of N-octyl monomers

The following is a representative procedure used for N-alkylation of the various 4-aminobenzoate ester monomers (see Scheme 1). The alkylation procedure was adopted from literature and proved to be successful for the N-alkylation step of all the monomers of interest. The synthetic procedures for the corresponding 4-aminobenzoate and initiator precursors is included in the supplementary information.

2.3.1 | Methyl 4-(octylamino) benzoate (1a)

Methyl 4-aminobenzoate (6.0 g, 38.9 mmol) and octanal (5.0 g, 38.9 mmol) were added to a round bottom flask with dry THF (200 ml). Acetic acid (2.9 ml, 51.3 mmol) and sodium triacetoxyborohydride (9.89 g, 46.7 mmol) were then added, and the flask was capped with a septum. The solution was stirred overnight at room temperature. The reaction was quenched by adding saturated sodium bicarbonate until the mixture became slightly basic. The product was isolated by extraction with ethyl acetate and washed with brine. After removal of the solvent, the resulting residue was recrystallized from methanol. Product: as white crystals; mp 89–90°C, (8.3 g, yield 81%). ^1H NMR (500 MHz, $CDCl_3$, δ): 7.85 (d, $J = 8.9$ Hz, 2H, ArH), 6.54 (d, $J = 8.9$ Hz, 2H, ArH), 4.13 (br, 1H), 3.83 (s, 3H), 3.14 (t, $J = 7.4$ Hz, 2H), 1.62 (q, $J = 7.4$ Hz, 2H), 1.42–1.22 (m, 10H), 0.88 (t, $J = 7.4$ Hz, 3H). ^{13}C NMR (125 MHz, $CDCl_3$, δ): 167.3, 152.1, 131.4, 117.6, 111.1, 51.3, 43.2, 31.7, 29.2, 29.16, 29.1, 27.0, 22.5, 14.0.; FTIR (ATR): $\nu = 3{,}376$ (Ar-NH-R), 2,946, 2,920, 2,849 (C—H), 1,678 (O—C═O), 1,596, 1,430, 1,190, 1,105, 832 cm^{-1}.

2.3.2 | Ethyl 4-(octylamino) benzoate (1b)

Ethyl 4-aminobenzoate (4.5 g, 27.2 mmol), octanal (3.5 g, 27.2 mmol), acetic acid (2.25 ml, 39.2 mmol), and sodium triacetoxyborohydride (6.9 g, 32.7 mmol) used. Product:

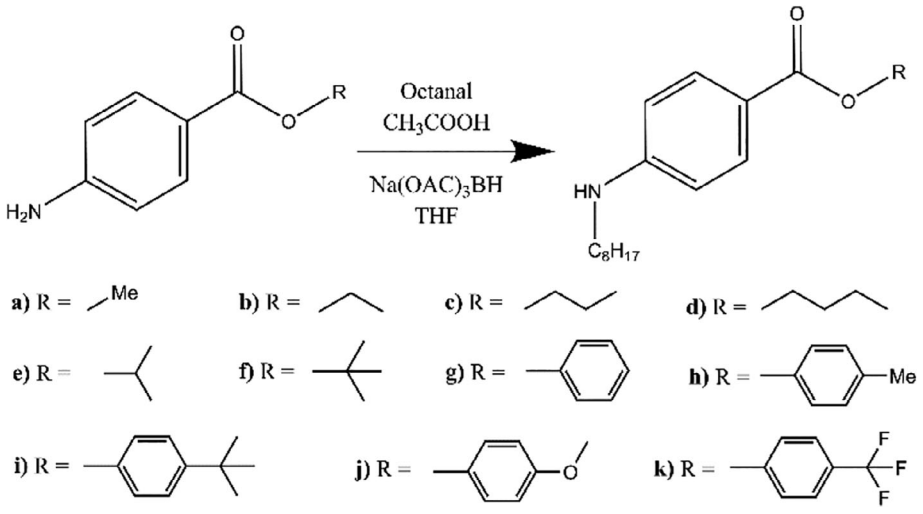

SCHEME 1 Alkylation procedure used to synthesize monomers with varying ester groups

as white crystals; mp 79–80°C, (5.1 g, yield 69%). ^{1}H NMR (500 MHz, $CDCl_3$, δ): 7.85 (d, J = 8.9 Hz, 2H, ArH), 6.54 (d, J = 8.9 Hz, 2H, ArH), 4.3 (t, J = 7.4 Hz, 2H), 4.1 (br, 1H), 3.14 (t, J = 7.4 Hz, 2H), 1.62 (q, J = 7.4 Hz, 2H), 1.42–1.22 (m, 13H), 0.88 (t, J = 7.4 Hz, 3H). ^{13}C NMR (125 MHz, $CDCl_3$, δ): 167.3, 152.1, 131.4, 117.6, 111.1, 51.3, 43.2, 31.7, 29.2, 29.16, 29.1, 27.0, 22.5, 14.0.; FTIR (ATR): ν = 3,368 (Ar-NH-R), 2,921, 2,852 (C—H), 1,679 (O—C═O), 1,600, 1,269, 1,106, 835 cm^{-1}.

2.3.3 | Propyl 4-(octylamino) benzoate (1c)

Propyl 4-aminobenzoate (4.0 g, 22.3 mmol), octanal (2.8 g, 22.3 mmol), acetic acid (1.95 ml, 33.5 mmol), and sodium triacetoxyborohydride (5.68 g, 26.8 mmol) used. Product: as white crystals; mp 66–67°C, (4.2 g, yield 65%).^{1}H NMR (500 MHz, $CDCl_3$, δ): 7.85 (d, J = 8.9 Hz, 2H, ArH), 6.54 (d, J = 8.9 Hz, 2H, ArH), 4.2 (br, 1H), 4.2 (t, J = 7.4 Hz, 2H), 3.16 (t, J = 7.4 Hz, 2H), 1.75 (m, J = 7.4 Hz, 2H), 1.42–1.22 (m, 10H), 1.0 (t, J = 7.4 Hz, 3H), 0.88 (t, J = 7.4 Hz, 3H). ^{13}C NMR (125 MHz, $CDCl_3$, δ): 167.3, 152.1, 131.4, 117.6, 111.1, 51.3, 43.2, 31.7, 29.2, 29.16, 29.1, 27.0, 22.5, 14.0.; FTIR (ATR): ν = 3,372 (Ar-NH-R), 2,953, 2,922, 2,852 (C—H), 1,677 (O—C═O), 1,600, 1,267, 1,169, 835, 771 cm^{-1}.

2.3.4 | Butyl 4-(octylamino) benzoate (1d)

Butyl 4-aminobenzoate (4.0 g, 20.7 mmol), octanal (2.6 g, 20.7 mmol), acetic acid (1.8 ml, 31.1 mmol), and sodium triacetoxyborohydride (5.3 g, 25.0 mmol) used. Product: as white crystals; mp 47–48°C, (4.3 g, yield 62%). ^{1}H NMR (500 MHz, $CDCl_3$, δ): 7.85 (d, J = 8.9 Hz, 2H, ArH), 6.54 (d, J = 8.9 Hz, 2H, ArH), 4.2 (br, 1H), 4.2 (t, J = 7.4 Hz, 2H), 3.16 (t, J = 7.4 Hz, 2H), 1.71 (q, J = 7.4 Hz, 2H), 1.62 (q, J = 7.4, 2 H) 1.42–1.22 (m, 12H), 0.95 (t, J = 7.4 Hz, 3H), 0.88 (t, J = 7.4 Hz, 3H). ^{13}C NMR (125 MHz, $CDCl_3$, δ): 167.3, 152.1, 131.4, 117.6, 111.1, 51.3, 43.2, 31.7, 29.2, 29.16, 29.1, 27.0, 22.5, 14.0.; FTIR (ATR): ν = 3,381 (Ar-NH-R), 2,954, 2,928, 2,855 (C—H), 1,682 (O—C═O), 1,600, 1,266, 1,168, 1,104, 831, 769 cm^{-1}.

2.3.5 | Isopropyl 4-(octylamino) benzoate (1e)

Isopropyl 4-aminobenzoate (4.0 g, 22.3 mmol), octanal (2.9 g, 22.3 mmol), acetic acid (1.9 ml, 33.5 mmol), and sodium triacetoxyborohydride (6.1 g, 29.0 mmol) used. Product: as white crystals; mp 90–91°C, (5.1 g, yield 80%).^{1}H NMR (500 MHz, $CDCl_3$, δ): 7.85 (d, J = 8.9 Hz, 2H, ArH), 6.54 (d, J = 8.9 Hz, 2H, ArH), 5.2 (m, J = 7.4 Hz, 1H), 4.1 (br, 1H), 3.16 (t, J = 7.4 Hz, 2H), 1.6 (q, J = 7.4, 2 H) 1.42–1.22 (m, 16H), 0.88 (t, J = 7.4 Hz, 3H). ^{13}C NMR (125 MHz, $CDCl_3$): δ = 167.3, 152.1, 131.4, 117.6, 111.1, 51.3, 43.2, 31.7, 29.2, 29.16, 29.1, 27.0, 22.5, 14.0.; FTIR (ATR): ν = 3,377 (Ar-NH-R), 2,956, 2,926, 2,854, 1,675 (O—C═O), 1,600, 1,270, 1,167, 1,100 cm^{-1}.

2.3.6 | *Tert*-butyl 4-(octylamino) benzoate (1f)

Tert-butyl 4-aminobenzoate (3.0 g, 15.5 mmol), octanal (2.0 g, 15.5 mmol), acetic acid (1.3 ml, 22.4 mmol), and sodium triacetoxyborohydride (3.95 g, 18.6 mmol) used. Product: as white crystals; mp 83–85°C, (2.6 g, yield 55%).^{1}H NMR (500 MHz, $CDCl_3$, δ): 7.85 (d, J = 8.9 Hz, 2H, ArH), 6.54 (d, J = 8.9 Hz, 2H, ArH), 4.5 (br, 1H), 3.16 (t, J = 7.4 Hz, 2H), 1.6 (q, J = 7.4 Hz, 2H) 1.55 (s, 9H), 1.42–1.22 (m, 10H), 0.88 (t, J = 7.4 Hz, 3H). ^{13}C NMR (125 MHz, $CDCl_3$, δ): 167.3, 152.1, 131.4, 117.6, 111.1, 51.3, 43.2, 31.7, 29.2, 29.16, 29.1, 27.0, 22.5, 14.0.; FTIR (ATR): ν = 3,377 (Ar-NH-R), 2,925, 2,854, 1,678 (O—C═O), 1,600, 1,288, 1,153, 1,106 cm^{-1}.

2.3.7 | Phenyl 4-(octylamino) benzoate (1g)

Phenyl 4-aminobenzoate (5.0 g, 23.5 mmol), octanal (3.62 g, 28.3 mmol), acetic acid (2.4 ml, 42.4 mmol), and sodium triacetoxyborohydride (7.18 g, 33.9 mmol) used. Product: as white crystals; mp 112–113°C, (7.3 g, yield 79%). ^{1}H NMR (500 MHz, $CDCl_3$, δ): 8.0 (d, J = 8.9 Hz, 2H, ArH), 7.4 (t, J = 8.1 Hz, 2H, ArH), 7.25 (t, J = 8.1 Hz, 1H, ArH), 7.18 (d, J = 8.1 Hz, 2H, ArH), 6.59 (d, J = 8.9 Hz, 2H, ArH), 4.2 (br, 1H), 3.2 (t, J = 7.4 Hz, 2H), 1.6 (q, J = 7.4 Hz, 2H), 1.42–1.22 (m, 10H), 0.88 (t, J = 7.4 Hz, 3H). ^{13}C NMR (125 MHz, $CDCl_3$, δ): 167.3, 152.1, 131.4, 117.6, 111.1, 51.3, 43.2, 31.7, 29.2, 29.16, 29.1, 27.0, 22.5, 14.0.; FTIR (ATR): ν = 3,288 (Ar-NH-R), 2,921, 2,852 (C—H), 1,681 (O—C═O), 1,594, 1,275, 1,163, 1,075, 742 cm^{-1}.

2.3.8 | p-Tolyl 4-(octylamino) benzoate (1h)

p-Tolyl 4-aminobenzoate (4.5 g, 20.0 mmol), octanal (2.8 g, 22.0 mmol), acetic acid (1.9 ml, 33.0 mmol), and sodium triacetoxyborohydride (6.1 g, 28.6 mmol) used. Product: as white crystals; mp 105–106°C, (6.1 g, yield 82%). ^{1}H NMR (500 MHz, $CDCl_3$, δ): 8.0 (d, J = 8.9 Hz,

2H, ArH), 7.2 (d, $J = 8.2$ Hz, 2H, ArH), 7.05 (d, $J = 8.2$ Hz, 2H, ArH), 6.61 (d, $J = 8.9$ Hz, 2H, ArH), 4.5 (br, 1H), 3.2 (t, $J = 7.4$ Hz, 2H), 2.35 (s, 3H), 1.6 (q, $J = 7.4$ Hz, 2H), 1.42–1.22 (m, 10H), 0.88 (t, $J = 7.4$ Hz, 3H). ^{13}C NMR (125 MHz, $CDCl_3$, δ): 167.3, 152.1, 1731.4, 117.6, 111.1, 51.3, 43.2, 31.7, 29.2, 29.16, 29.1, 27.0, 22.5, 14.0.; FTIR (ATR): ν = 3,369 (Ar-NH-R), 2,919, 2,842 (C—H), 1,694 (O—C═O), 1,595, 1,350, 1,264, 1,056, 835 cm^{-1}.

2.3.9 | *Tert*-butylphenyl 4-(octylamino) benzoate (1i)

Tert-butyl 4-aminobenzoate (5.0 g, 18.6 mmol), octanal (2.4 g, 18.6 mmol), acetic acid (1.6 ml, 27.8 mmol), and sodium triacetoxyborohydride (5.1 g, 24.2 mmol) used. Product: as white crystals; mp 130–131°C, (5.7 g, yield 80%).^{1}H NMR (500 MHz, $CDCl_3$, δ): 8.0 (d, $J = 8.9$ Hz, 2H, ArH), 7.40 (d, $J = 8.9$ Hz, 2H, ArH), 7.1 (d, $J = 8.9$ Hz, 2H, ArH), 6.58 (d, $J = 8.9$ Hz, 2H, ArH), 4.2 (br, 1H), 3.2 (t, $J = 7.4$ Hz, 2H), 1.6 (q, $J = 7.4$ Hz, 2H), 1.42–1.22 (m, 19H), 0.88 (t, $J = 7.4$ Hz, 3H). ^{13}C NMR (125 MHz, $CDCl_3$, δ): 165.6, 152.7, 149.0, 148.2, 132.3, 126.3, 121.2, 117.2, 111.4, 99.9, 43.5, 34.5, 31.8, 31.5, 29.45, 29.40, 29.33, 27.2, 22.75, 14.2.; FTIR (ATR): ν = 3,371 (Ar-NH-R), 2,956, 2,929, 2,853 (C—H), 1,692 (O—C═O), 1,599, 1,356, 1,265, 1,163, 1,061, 835, 808 cm^{-1}.

2.3.10 | p-Methoxyphenyl 4-(octylamino) benzoate (1j)

p-Methoxyphenyl 4-aminobenzoate (6.0 g, 24.7 mmol), octanal (3.2 g, 24.7 mmol), acetic acid (2.2 ml, 37.0 mmol), and sodium triacetoxyborohydride (6.8 g, 32.1 mmol) used. Product: as white crystals; mp 130–131°C, (7.2 g, yield 82%).^{1}H NMR (500 MHz, $CDCl_3$, δ): 8.0 (d, $J = 8.9$ Hz, 2H, ArH), 7.1 (d, $J = 8.9$ Hz, 2H, ArH), 6.9 (d, $J = 8.9$ Hz, 2H, ArH), 6.58 (d, $J = 8.9$ Hz, 2H, ArH), 4.2 (br, 1H), 3.8 (s, 3H), 3.18 (t, $J = 7.4$ Hz, 2H), 1.6 (q, $J = 7.4$ Hz, 2H), 1.42–1.22 (m, 10H), 0.88 (t, $J = 7.4$ Hz, 3H). ^{13}C NMR (125 MHz, $CDCl_3$, δ): 165.8, 157.1, 152.6, 144.9, 132.3, 122.7, 119.2, 114.5, 111.4, 55.7, 43.5, 31.8, 29.45, 29.40, 29.33, 27.2, 22.75, 14.2.; FTIR (ATR): ν = 3,378 (Ar-NH-R), 2,928, 2,921, 2,856 (C—H), 1,687 (O—C═O), 1,597, 1,349, 1,282, 1,165, 1,074, 836, 765 cm^{-1}.

2.3.11 | Triflurомethylphenyl 4-(octylamino) benzoate (1k)

Triflurомethylphenyl 4-aminobenzoate (5.0 g, 17.8 mmol), octanal (2.3 g, 17.8 mmol), acetic acid (1.5 ml, 26.7 mmol), and sodium triacetoxyborohydride (4.9 g, 23.1 mmol) used. Product: as white crystals; mp 129–130°C, (4.9 g, yield 70%). ^{1}H NMR (500 MHz, $CDCl_3$, δ): 8.0 (d, $J = 8.9$ Hz, 2H, ArH), 7.7 (d, $J = 8.9$ Hz, 2H, ArH), 7.3 (d, $J = 8.9$ Hz, 2H, ArH), 6.59 (d, $J = 8.9$ Hz, 2H, ArH), 4.25 (br, 1H), 3.2 (t, $J = 7.4$ Hz, 2H), 1.6 (q, $J = 7.4$ Hz, 2H), 1.42–1.22 (m, 10H), 0.88 (t, $J = 7.4$ Hz, 3H). ^{13}C NMR (125 MHz, $CDCl_3$, δ): 164.9, 152.9, 132.5, 126.7 (q, $J = 3.8$ Hz) (C-F), 122.5, 116.2, 111.5, 43.2, 31.7, 29.2, 29.16, 29.1, 27.0, 22.5, 14.0. ^{19}F NMR 1 peak; FTIR (ATR): ν = 3,376 (Ar-NH-R), 2,952, 2,924, 2,854 (C—H), 1,698 (-CO-O), 1,598, 1,320, 1,272, 1,159, 1,120, 1,058, 833, 761 cm^{-1}.

2.4 | Synthesis of initiator

2.4.1 | Phenyl 4-(dimethyl carbamoyl) benzoate (DMA-P Initiator)

In a 100 ml round bottom flask, with a stir bar, was placed 4-(phenoxycarbonyl)benzoic acid (1.1 g, 4.5 mmol) and $SOCl_2$ (11 ml, 150 mmol). The mixture was refluxed until the acid dissolved, producing the acid chloride. Excess $SOCl_2$ was removed under vacuum. The remaining acid chloride was dissolved in anhydrous DCM (30 ml). A solution of dimethylamine (2 M in THF) (2.73 ml, 5.5 mmol), triethylamine (0.7 ml, 5.0 mmol), and DCM (20 ml) was prepared and added slowly to the acid chloride. The mixture was refluxed for 1 hr. The solvent was then removed under vacuum, the residue was dissolved in ethyl acetate and passed through a short column (eluted with ethyl acetate). After removal of the solvent and drying under vacuum, no further purification was necessary. Product: as white crystals; mp 111–112°C, (0.86 g, yield 70%).^{1}H NMR (500 MHz, $CDDl_3$, δ): 8.2 (d, $J = 8.1$ Hz, 2H, ArH), 7.54 (d, $J = 8.2$ Hz, 2H, ArH), 7.42 (t, $J = 8.0$ Hz, 2H, Ar H), 7.27 (t, $J = 8.0$ Hz, 1H, ArH), 7.21 (d, $J = 8.0$ Hz, 2H, ArH), 3.1, (s, 3H) 2.97 (s, 3H) (N-CH_3); ^{13}C NMR (150 MHz, $CDCl_3$, δ): 170.5, 164.6, 150.9, 141.4, 130.46, 130.40, 129.6, 127.3, 126.1, 121.7, 39.4, 35.4; FTIR (ATR): ν = 3,085, 2,920, 1724 (O—C═O), 1,616 (N—C═O), 1,393, 1,265, 1,085, 876, 720 cm^{-1}.

2.5 | Polymerization methods

2.5.1 | Solubility experiments

A representative procedure is outlined below for the methyl ester monomer (1a) at room temperature, where the only difference between other monomer experiments

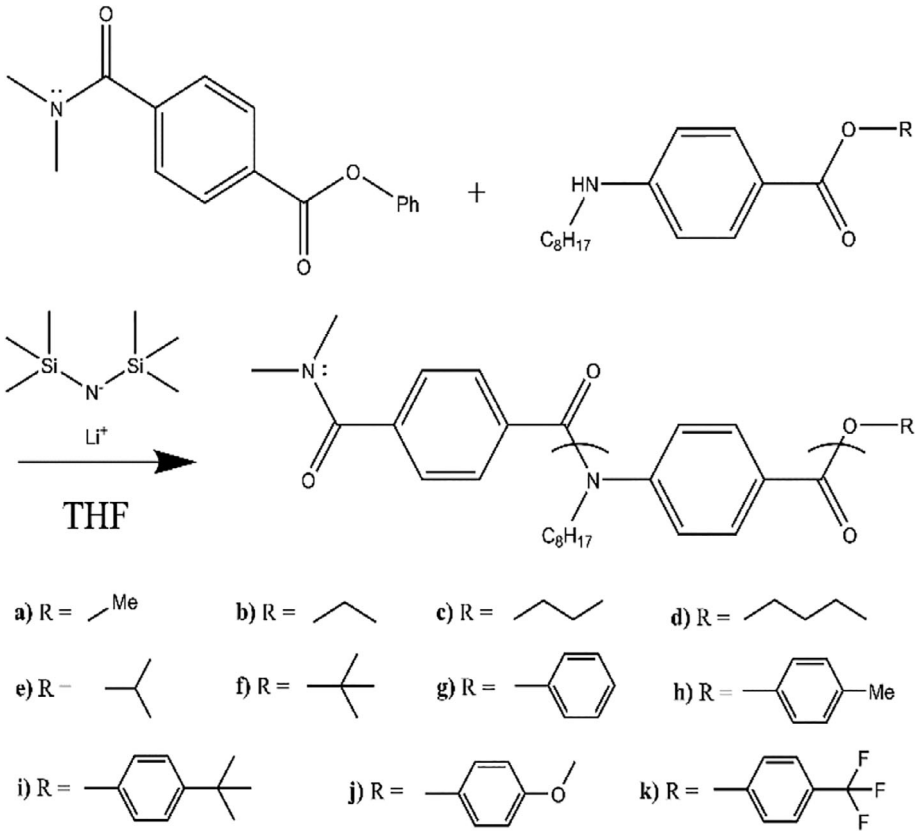

SCHEME 2 Polymerization scheme using DMA-P initiator and octyl monomers with varying ester R substituents

is the nature of the monomer and the temperature of the polymerization, with the molar amounts remaining the same. A typical polymerization procedure utilizing the DMA-P initiator and the monomer of interest is depicted in Scheme 2.

The monomer 1a (0.264 g, 1.0 mmol) and DMA-P initiator (6.8 mg, 0.025 mmol) were placed in a flask, purged with argon for 5 min, followed by the addition of THF (20 ml) via syringe and needle. The LiHMDS base (1.1 ml, 1.1 mmol) was then injected and the solution was stirred for 12 hr at 20°C. Qualitative solubility observations were collected by observing the opacity of the resulting solution.

The polymer was then isolated via extraction with DCM, purified by washing with a NaOH/brine solution, dried over $MgSO_4$, and isolated by removing the solvent and by-products under vacuum before further drying in a vacuum oven at 60°C for 2 hr.

2.5.2 | Kinetics experiments

A representative procedure is outlined below for the methyl ester monomer (1a) at room temperature, where the only difference between other monomer experiments is the nature of the monomer and temperature of the polymerization, with the molar amounts remaining the same.

The monomer 1a (0.132 g, 0.5 mmol) and DMA-P initiator (3.4 mg, 0.025 mmol) were placed in a flask, purged with argon for 5 min, followed by addition of THF (10 ml) via syringe and needle. The resulting solution was then brought to the desired temperature—a room temperature bath was achieved with a monitored water bath, an ice bath was used for 0°C, a saturated brine bath was used for a temperature of −20°C, dry ice and acetonitrile was used for −48°C, and dry ice/acetone was used for the −78°C reaction temperature. The LiHMDS base (0.6 ml, 0.6 mmol) was then injected, thus starting the reaction. The polymerization was then allowed to proceed for the desired amount of time followed by removal of a 1 ml aliquot for analysis, which was quenched by addition to an aqueous saturated ammonium chloride solution. The polymer workup remained the same as discussed above to isolate the converted polymer. NMR and GPC experiments were used to determine subsequent conversion, molecular weights, and molecular weight distributions.

2.5.3 | Computation modeling parameters

All computations were performed at the high-performance computing facility accessible through the Colorado School of Mines. The Gaussian 09 package was

utilized for density functional theory (DFT) calculations performed during this study.[18] Geometry optimizations were performed using the 2006 version of the Global hybrid Minnesota functional (M06-2X) and the split valance polarized basis set 6–31 + G(d).[19,20,21] To mimic impact of the solvent, implicit solvation of THF was incorporated into the calculations using the integral equation formalism variant polarizable continuum mode (IEFPCM).[22] The minimum energy structures were characterized by the absence of any imaginary frequencies while the transition states were confirmed by the presence of an imaginary frequency corresponding to the mode of interest. Partial atomic charges were computed using a Natural Bond Orbital (NBO) analysis.[23] Activation energies and reaction rates for the polymer growth mechanism were obtained using the previously mentioned calculations in the KisThelP package.[24] Coordinates for all structures presented in this study are available in the supporting information.

3 | RESULTS AND DISCUSSION

The clear majority of literature on application of the CGC technique involves the polymerization of methyl ester monomers (1a), which have proved to be mostly successful in producing defined polymers and also produces low-boiling point byroducts.[14–16,25–32] Based on this literature, we hypothesized that the methyl monomer would be a good candidate for the preparation of aromatic polyamide brushes via CGC polymerization in our original work.[11] However, in this work it was observed that control over the polymerization was only achieved up to a degree of polymerization (DP) of ~80, which also corresponds to literature studying solution polymerizations of the same monomer.[14] The proposed mechanism for CGC suggests that control over the polymerization is primarily achieved when the end group of the polymer is selectively available for reaction with the amide anion nucleophile. In our previous polymer brush paper, it was observed that during the polymerization of the methyl ester monomer, the solution turned from a clear yellow solution to a very cloudy, almost slurry, toward the completion of the reaction. As formation of the insoluble product corresponded to loss of control in the polymerization, we hypothesized that control is lost because of either the diminished solubility of the produced polymer or insoluble condensation by-products.

To obtain better control over the polymer molecular weight and produce polymers of low polydispersity, it is important to understand the CGC polymerization mechanism. A depiction of the polymerization propagation reaction is shown in Scheme 3. Before the monomer can add to the active polymer end group, it must be deprotonated by the strong non-nucleophilic base LiHMDS. The reactive monomer can then add to either the initiator or the end group of a growing polymer's ester group to give a tetrahedral intermediate transition state. This intermediate can then either return to the original reactants or rearrange to eliminate the ester alkoxide, leaving the polymer chain with one additional monomer and the lithium alkoxide as the by-product. Traditionally, discussion of the CGC mechanism has focused solely on the reactivity or electrophilicity of the carbonyl carbon of the ester monomer. However, Scheme 3 highlights the importance of not only the electrophilicity of the carbon of the ester carbonyl group but also the basicity of the ester alkoxide and the solubility of the lithium alkoxide in propagation of the polymer chain. Therefore, it is important to study the effects of these factors in the polymerization system, which has not occurred to date, to truly understand the mechanism and to maintain control over the CGC polymerization. Common to each of these factors is the structure of the monomer ester group, thus designing polymers using monomers with different ester groups should allow for a

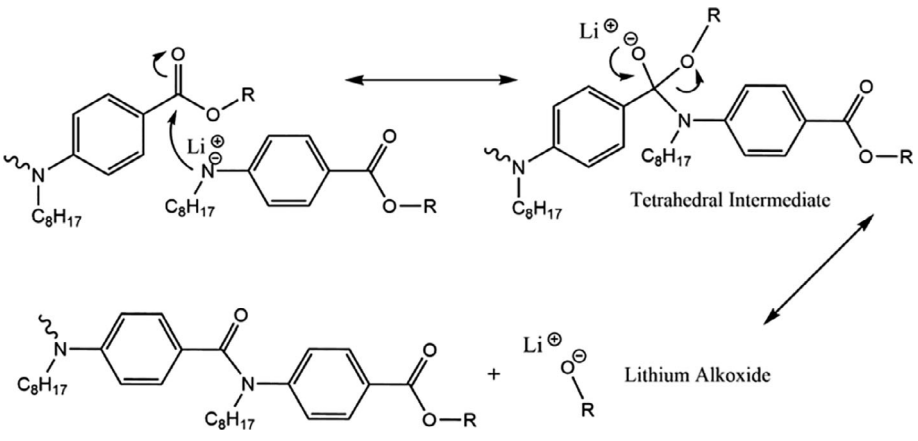

SCHEME 3 Polymerization mechanism for nucleophilic acyl substitution at the ester carbonyl group during addition of monomer to the propagating polymer chain

better understanding of the factors that affect the formation of well-defined polymers using the CGC technique by examining the solubility of the produced by-products and reactivity of the ester polymer end group.

3.1 | Solubility of lithium alkoxides and phenoxides

To address the solubility issue attributed to CGC polymerization of the methyl ester monomer, the solubility of different lithium alkoxides and phenoxides was investigated. Changing the ester substituent on the monomer will allow for the formation of different lithium alkoxides after the nucleophilic acyl substitution reaction at the polymer end group. The ester substituent also has the potential to change the reactivity and solubility of both the polymer end group and the resulting lithium alkoxides. The preliminary study used to investigate the solubility of the alkoxide produced from the different ester monomers was to recreate the conditions of post-polymerization by deprotonating the candidate parent alcohols, using LiHMDS, and create the lithium alkoxide in a THF solution. For example, the solution of lithium methoxide was prepared by addition of LiHMDS to a THF solution of methanol at the same concentration, as they would be in the polymerization solution. The results showed that the lithium methoxide salt was indeed insoluble, as it produced a cloudy suspension under these conditions. However, it was observed that all other aliphatic alcohols of interest: ethyl, propyl, butyl, isopropyl, and tert-butyl, yielded much clearer solutions under the same conditions, suggesting they produced more soluble lithium alkoxides in THF. In addition, we also investigated various lithium phenoxides as potential ester monomer candidates. Phenol, along with para-substituted phenols (p-cresol, 4-tert butyl phenol, 4-methoxy phenol, and 4-trifluoromethyl phenol), were mixed with 1 equivalent of LiHMDS in THF. The results demonstrated that all systems produced clear solutions, suggesting that lithium phenoxide salts also have good solubility in THF. There are few examples examining the solubility of lithium alkoxides and phenoxides in literature. Kamienski and Lewis have conducted the most detailed study of the solubility of lithium alkoxides, concluding that alkoxides with branching have increased solubility in hydrocarbon solvents and ethers but lower solubility in alcohols.[33] While this work also demonstrated that the solubility of straight chain alkoxides in ethers and hydrocarbons is low, they did observe a slight increase in solubility as the chain length of the alkoxide increases.

Understanding the reasons for the variation in the solubility of the different lithium alkoxides and phenoxides is a difficult and complex task. While Kamienski attributed the differences in solubility in hydrocarbon and ether solvents to different degrees of polymerization or aggregation of the alkoxides, Arnett demonstrated that there was no obvious relationship between the aggregation number of lithium alkoxides and the basicity of the corresponding anion and, in conjunction with the observation that there was equilibria between different aggregation states, concluded that there are only small differences between the relative stabilities of different aggregation states.[34] Despite the complexity of this area, it was decided in order to proceed with the current investigation, only monomers that produced soluble lithium alkoxides or phenoxides, based upon the previous solubility tests, would be prepared, and used to investigate the effect of different leaving groups on the CGC polymerization performance.

3.2 | Polymerization of alkyl ester derivatives

3.2.1 | Solubility

The polymerization of the n-alkyl ester monomers 1b-1d all yielded solutions that appeared optically very similar to the methyl ester monomer 1a, producing opaque solutions despite the hypothesis that increasing the length of the alkyl chain would produce more soluble lithium alkoxides and the results of the lithium alkoxide solubility tests described above. However, it was observed that the longer the alkyl chain of the ester, the less cloudy the final polymerization solution, although all the solutions had some degree of opacity. In comparison, the resulting polymerization solutions for the branched isopropyl and tert-butyl ester monomers 1e and 1f, respectively, produced clear solutions. The branched ester results demonstrate that while the branched alkoxides follow the observations of the previous alkoxide solubility tests, the n-alkyl alkoxides do not, in that they produced insoluble products. However, they do agree with observations in literature.

The reason for the varying solubility results for the alkyl esters is most likely because the aggregation states for lithium alkoxides are strongly dependent on temperature, concentration, and solvent type. These results suggest that the presence of monomer and/or polymer in solution changes the solubility of the alkoxides, resulting in some degree of insolubility for all the n-alkyl alkoxides, however, good solubility for the branched alkoxides was maintained.

TABLE 1 Comparison between the polymerization results of methyl and ethyl ester substituents base LiHMDS

Ester	Conv. (%)	M_n (NMR) (g/mol)	PDI (GPC)	k_p at 20°C ($M^{-1}.s^{-1}$)
Methyl	100	8,240	1.09	0.28
Ethyl	95	8,040	1.11	0.11

3.2.2 | Kinetics

To investigate the properties of the alkyl ester monomers further, kinetic studies were performed. These studies demonstrated that even though the straight chain ester monomers polymerize under the conditions utilized, they would all reach a limiting conversion, where the extent of conversion decreased with increasing alkyl chain length. In a comparison between the methyl and ethyl ester monomers (Table 1), it is evident that under the same reaction conditions of 12 hr at 20°C, the ethyl monomer only reaches 95% conversion, with slightly higher PDI. These results are similar to previous results in literature for a meta monomer system investigating the utilization of ethyl esters.[15] The kinetics performed on the ethyl ester also shows that the ethyl ester proceeds at a slightly slower rate (Table 1).

The polymerization of the monomers that contain the isopropyl and tert-butyl esters (1e and 1f) yielded interesting results. Based on kinetic studies, the isopropyl monomer (1e) polymerizes at a significantly slower rate than the n-alkyl esters, despite maintaining solubility throughout the polymerization. However, after reaching a conversion of 38% the reaction would stop. It was also observed that the tert-butyl ester monomer (1f) had no reactivity towards polymerization, with no conversion achieved even after a reaction period of 2 days or by conducting the reaction under reflux conditions.

The variation in kinetic results of the alkyl ester monomers can be explained by both the sterics and the relative basicity of the alkoxide produced as part of the nucleophilic acyl substitution propagation reaction. In terms of sterics, it is hypothesized that increased branching on the ester alkoxide increases the activation energy for formation of the tetrahedral intermediate due to crowding around the electrophilic carbon of the carbonyl as the nucleophile approaches. In addition, the rate of aminolysis of the ester end group of the polymer chain is dependent on the relative basicity of the alkoxide leaving group, with breakdown of the tetrahedral intermediate to the amide product and alkoxide by-product favored by a less basic alkoxides or more acidic conjugate acids of the alkoxide leaving group (see Table 2). The pKa of the conjugate acid of tert-butoxide, tert-butanol, has the highest pKa (19.2) of all the alkoxides studied, with a gradual decrease in pKa observed with a decrease in both branching and n-alkyl chain length to the simplest alkoxide, methanol at a pKa of 15.5.[35] Both of these factors contribute to the decreased reactivity of the two branched ester derivatives, with the increased steric hindrance and high pKa of the tert-butyl group producing a system essentially inert to polymerization under the conditions used.

TABLE 2 pKa values of conjugate acids corresponding to the lithium alkoxides produced as by-products

Conjugate acid	pKa[a] at 25°C in water
Tert-butanol	19.2
Isopropanol	17.1
n-butanol	16.1
n-propanol	16.1
Ethanol	16.0
Methanol	15.5
CH_3O-phenol	10.8
$(CH_3)_3C$-phenol	10.4
CH_3-phenol	10.1
Phenol	9.9
CF_3-phenol	8.7

[a]Values from Perrin.[29]

Based on the above results, it was concluded that the alkyl ester monomers produce polymer solutions containing insoluble by-products and/or have low polymerization rates, both of which limit the ability to achieve a well-controlled polymerization and produce well-defined polymers. As a result, our attention was subsequently focused on utilizing the phenyl ester monomers.

3.3 | Polymerization of phenyl esters derivatives solubility

The phenyl ester monomer (1g) has been previously utilized to prepare a variety of aromatic polyamide structures by CGC polymerization and is typically the ester of choice with these polymerizations, due to its relatively high reactivity, compared with the methyl ester.[29,36–39] In addition, the preliminary solubility studies discussed above demonstrated that the resulting solutions for all the tested phenoxides, derived from the phenyl ester

monomers (1g-1k), were soluble. Based on these factors, the effectiveness of the different phenyl ester monomers in CGC polymerizations was investigated.

Initial polymerizations demonstrated that the phenyl ester monomers (1g-1k) all produced clear solutions throughout the course of the reaction, indicating that both the polymer and the condensation by-products formed were soluble under these conditions. Unlike lithium alkoxides, there is very little data in the literature regarding the solubility of lithium phenoxides. Arnett demonstrated the solubility of a wide range of phenol derivatives in THF, after deprotonation with LiHMDS, while studying the aggregation numbers of a variety of lithium salts.[34] In this study, all the lithium phenoxides examined, except that produced after deprotonation of methyl 4-hydroxybenzoate, were soluble in THF at a concentration of 0.10 M. The excellent solubility of all components of the polymerization process when using phenyl ester monomers allowed for a kinetic study to determine the control over the CGC polymerization reaction without having to be concerned with competing precipitation reactions.

3.3.1 | Kinetics

Kinetic studies were performed on the phenyl ester monomers to examine the effect of substitution on the reactivity of the different monomers (1g-1k). Each experiment consisted of taking four samples at a given temperature to monitor conversion using NMR. As can be seen in Figure 1, the molecular weight obtained using NMR shows good agreement with the theoretical molecular weights and demonstrates a linear relationship when plotted against the conversion of monomer, indicating a constant concentration of chains in the polymerization system.

The kinetic semi-logarithmic plots of conversion versus time were obtained by determining the conversion throughout the polymerization (Figure 2). Specifically, the monomer conversion was computed using the ratios of monomer and polymer NMR proton signals adjacent to the nitrogen amide (polymer) or amino (monomer) group on the benzene ring. Figure 2 shows that a linear relationship was obtained for each system at a reaction temperature of −20°C, indicating a constant number of active species in the polymerization. Results for the monomers not shown are can be found in the supporting information (Figure S5). The reaction temperature of −20°C was chosen as it was the lower end of the temperature range for maintaining a controlled polymerization for the slowest methyl ester monomer (1a), while also being the upper temperature range for control of the fastest trifluoromethyl phenyl ester monomer (1k). From the semi-logarithmic plots, propagation rate constant (k_p) values were calculated (Figure 2) and demonstrate that

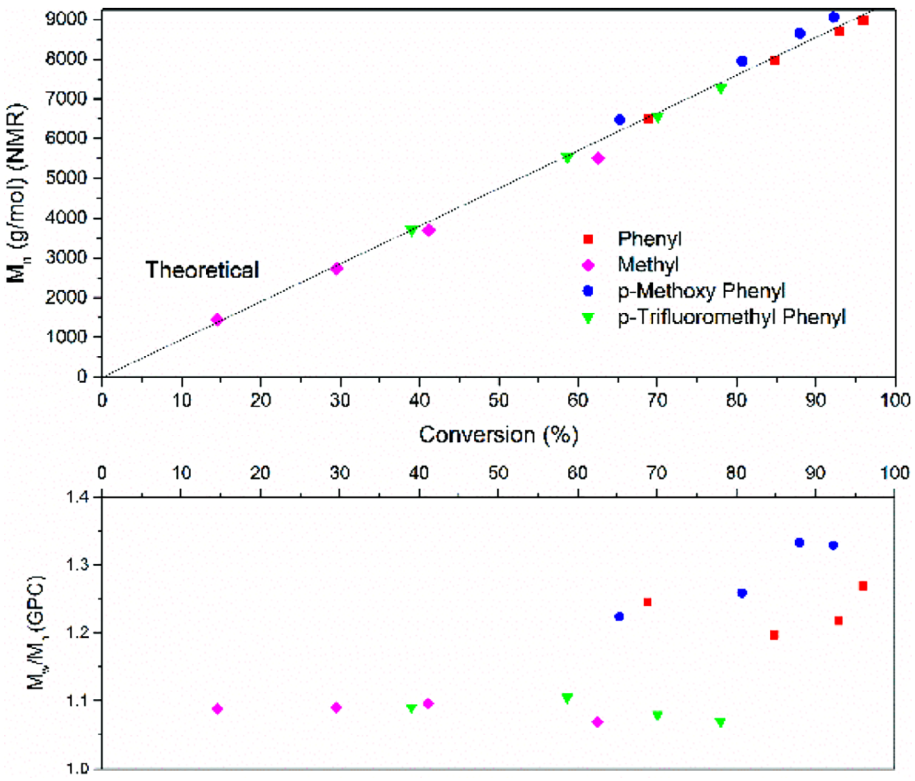

FIGURE 1 Relationship between number average molecular weight (M_n) and conversion and the molecular weight distribution and conversion for four of the studied monomers [Color figure can be viewed at wileyonlinelibrary.com]

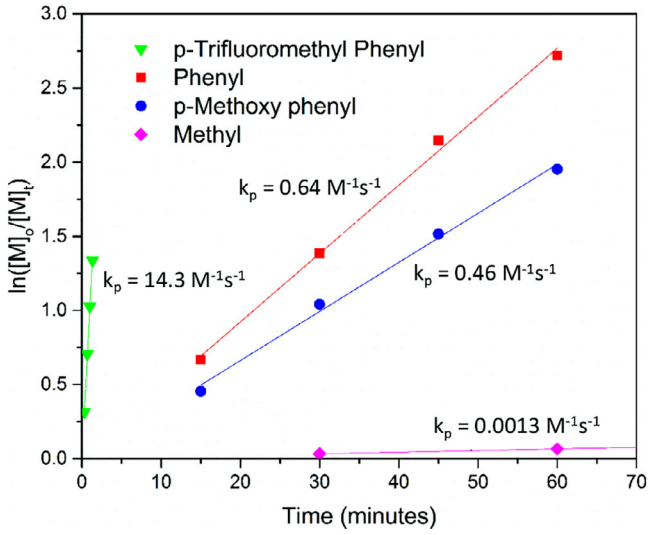

FIGURE 2 Polymer kinetics studied for various ester monomers at −20°C. The experimental propagation rate constants were calculated from the slope of the plots and the initiator concentration. Error in k_p values is ±0.01 M^{-1} s^{-1} [Color figure can be viewed at wileyonlinelibrary.com]

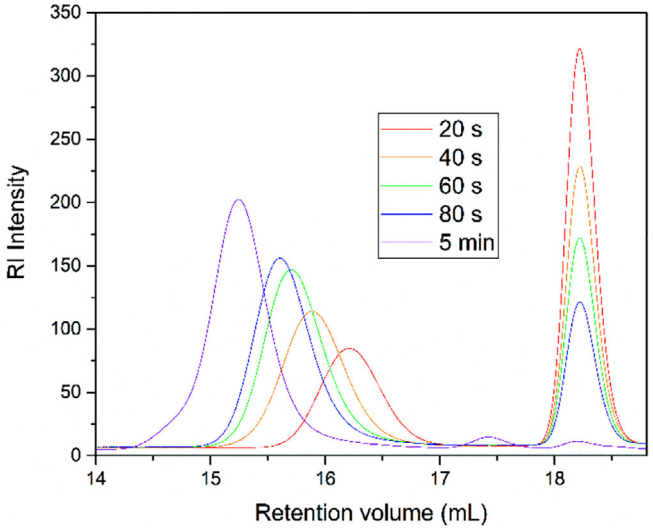

FIGURE 3 GPC traces demonstrating molecular weight and molecular weight distribution evolution for the trifluoromethyl phenyl ester monomer (1 k) at −20°C [Color figure can be viewed at wileyonlinelibrary.com]

the trifluoromethyl phenyl ester monomer is the most reactive with a k_p = 14.3 M^{-1} s^{-1}, which is three orders of magnitude faster than the slowest monomer, the methyl ester, with a k_p = 0.013 M^{-1} s^{-1}. The molecular weight distribution with time was also monitored via GPC. Figure 3 shows the molecular weight distributions for the p-trifluoromethyl phenyl ester monomer (1k) as a function of time at −20°C. These traces show monomodal peaks throughout the course of the reaction and that the polymer maintains a narrow molecular weight distribution with the PDI values ranging from 1.09 to 1.11. The peak at a retention volume near 18 ml, is due to monomer and shows a decrease with time as the monomer in the system is consumed and the reaction reaches completion in under 5 min.

The focus of the kinetic studies was to study how the para substituents on the phenyl ester monomer affects the overall polymerization process. Conventional understanding in the literature is that well defined CGC polymers are prepared by converting the traditional step-growth process into a chain-growth process by deactivating the ester substituent on the monomer.[7,9] This is achieved by deprotonation of the amine on the monomer by strong base, with the resulting amide anion donating electron density to the ring and effectively making the carbonyl carbon of the ester less electrophilic and, hence, less reactive to nucleophilic acyl substitution. Decreasing the reactivity of the carbonyl carbon is assumed to limit the monomer-monomer reactions typically observed in step-growth polymerizations. Based on the results in this study, the reactivity of the monomer towards nucleophilic acyl substitution is a function of more than just the carbonyl electrophilicity; it is also strongly influenced by the basicity of the leaving alkoxide.

As discussed previously, Scheme 3 depicts the nucleophilic acyl substitution mechanism for addition of monomer to the polymer end group. From this mechanism, it is apparent that formation of the tetrahedral transition state has an energy barrier that is associated with the reactivity and, hence, the kinetics, of the polymerization system. The process where the alkoxide is eliminated from the tetrahedral intermediate plays a significant role on how efficiently the process happens. It is hypothesized that, the more stable the negative charge on the alkoxide, the more easily it is eliminated from the intermediate complex, increasing the overall reaction rate. The stability mentioned herein refers to how well the negative charge is delocalized and stabilized and can be related to the pKa of the alkoxides conjugate acid, or the parent alcohol (Table 2).

It is apparent from Table 2 that the pKa is highest for the bulkiest alkyl alcohol, tert-butanol with a value of 19.2, followed by isopropanol, linear alkanes, ethanol, and finally methanol at 15.5. This can be explained by the more electron donating character of the alkyl groups destabilizing the charge, making the deprotonation process less favorable. There is a large jump in pKa from methanol (15.5) to the various phenol derivatives (starting at 10.8), due to the ability of the phenyl structures to stabilize the resulting negative charge through resonance. The pKa for the para-substituted phenol

derivatives drops with increasing electron withdrawing character of the substituent, to a pKa of 8.7.

3.3.2 | Determination of activation energies

Kinetic data was collected for all the phenyl ester derivative monomers, along with the methyl monomer (1a), since it was the only alkyl ester monomer where full conversion was achieved. From this data, the experimental k_p values were calculated for each monomer at three temperatures. For all the monomers, excluding the trifluoromethyl phenyl monomer (1 k), polymerizations were run at 20, 0, and −20°C. These temperatures were chosen because the kinetics for these monomers in this temperature range were slow enough to allow samples to be taken. The temperatures chosen for the trifluoromethyl phenyl monomer (1k) were −20, −48, and −78°C, due to the very high reactivity of this monomer. It was found that above these temperatures, the reaction was complete in less than a minute and the polymers produced had high PDIs, near 1.7–1.8, demonstrating a lack of control in the CGC polymerization process. The kinetic data was then used to determine the activation energy (E_a) of the various reactions via the Arrhenius relationship (Figure 4). Results for the monomers not shown are can be found in the supporting information (Figure S5). A complete list of activation energies is summarized in Table 3. The E_a values obtained from the kinetic experiments closely follow the observed reactivity trend for the different monomers.

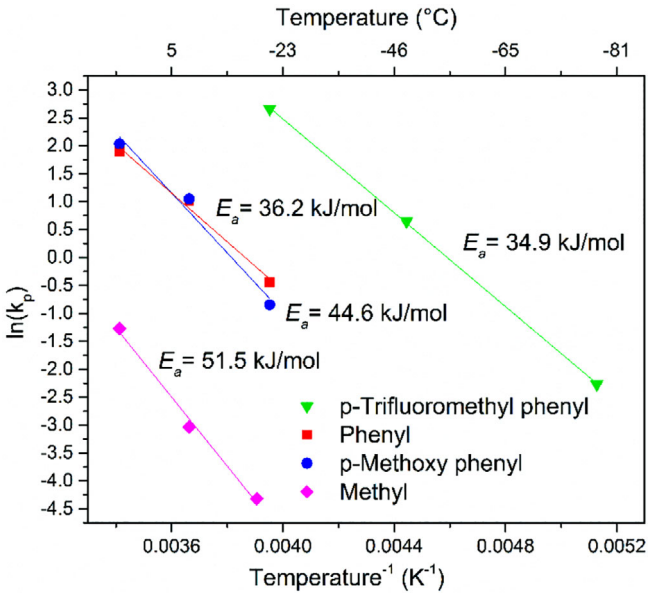

FIGURE 4 Arrhenius relationships for the various ester monomers. The activation energies (E_a) were calculated from the slopes of the plots. Error in the E_a values is ±0.1 kJ/mol [Color figure can be viewed at wileyonlinelibrary.com]

The general reactivity trend of the esters reported above agrees, to a certain degree, with literature on the reactivity of small molecule esters with various nucleophiles.[40,41] The hydrolysis of esters has been studied extensively and it has been observed that the O-substituent of the ester plays a key role in determining its reactivity. Mitton and coworkers reported that, for hydrolysis of various esters, the fate of the leaving groups also depends on the relative basicity of the alkoxide after elimination from the tetrahedral intermediate adduct.[40] In more relevant studies, Menger and coworkers examined the aminolysis of esters in protic solvents and demonstrated that the rate determining step of the reaction is related to the stability of the alkoxide leaving group.[41] In addition, recent theoretical work investigating the aminolysis reaction of methylamine with methyl acetate proposed that a mechanism that bypasses the tetrahedral intermediate might exist. The two separate mechanisms put forward were a direct substitution reaction, where the exchange occurs via a concerted pathway, and an exchange that is assisted by a 2(1H)-pyridone catalyst.[42,43] The conclusion of this work suggest that there are alternative mechanisms that could explain the behavior of aminolysis reactions and the mechanisms have the potential to be quite complex. However, these studies were conducted with the protonated amine exchanging

TABLE 3 Arrhenius data including the slope, intercept, and calculated activation energies for the monomers examined

Funct. group	Slope (K)	Intercept	Activation energy (kJ/mol)
F_3C-Ph	4,197.6	19.3	34.9
Phenyl	4,359.5	16.8	36.2
H_3C-Ph	4,424.6	17.6	36.8
$(H_3C)_3C$-Ph	4,847.8	18.9	40.3
H_3CO-Ph	5,364.1	20.5	44.6
Methyl	6,188.3	51.5	51.5

Note: Error in the calculated activation energies is ±0.1 kJ/mol.

with the more stable leaving alcohol and there is very little discussion in the literature of the mechanisms of lithiated basic aminolysis under aprotic conditions. Despite the agreement between the results obtained here and the literature on nucleophilic acyl substitution using small molecules, this study represents the first detailed investigation on the effect of the ester leaving group on the nature of the CGC polymerization process.

3.4 | Computational modeling: Activation energies and charges

To gain a better understanding of the experimental results presented above, DFT calculations were performed on the CGC polymerization mechanism. The octyl group in the monomers was replaced with a methyl group along with a truncated species 4.3 to reduce the computational cost (Scheme 4). An NBO analysis was performed to gain insight on the electrophilic nature of the ester carbonyl groups involved in the formation of the tetrahedral intermediate and the elimination of the alkoxide product. Additionally, transition state calculations were performed to determine the roles electrophilicity of the carbonyl carbon, formation of the tetrahedral intermediate, and stability of the leaving group play in the reaction energetics. Moreover, transition state calculations were also used to obtain the activation barriers for the overall mechanism. To the best of our knowledge, this is the first computational study of the CGC polymerization system for the synthesis of aromatic polyamides.

3.4.1 | Reaction energetics

As shown in Scheme 3, the addition of monomer in the CGC polymerization mechanism goes through two steps:

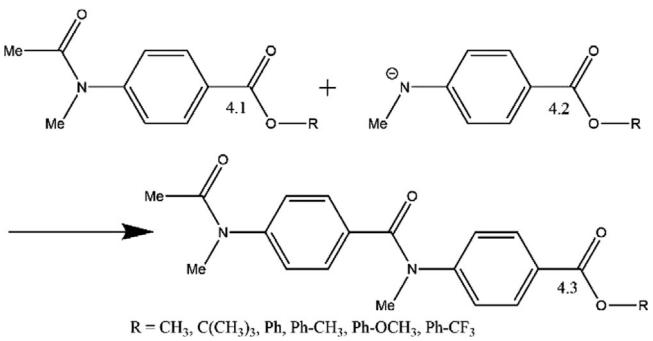

SCHEME 4 Model system employed for computational studies. The charges of the three esters of interest were calculated for the phenyl ester monomer system, along with the charges for varied esters. The numbers 4.1, 4.2, and 4.3 are used to define the species in the discussion

(a) attack of the nucleophile on the ester carbonyl center to form the tetrahedral intermediate, and (b) decomposition of the tetrahedral intermediate to produce the polymer product with one addition monomer unit and the alkoxide leaving group. The transition states for both of these steps were calculated for the alkyl monomers 1a and 1f, and the phenyl monomers 1g, 1h, 1j, and 1k (Scheme 2). The calculated reaction energetics are summarized in Figure 5 (Table S1 in the supporting information contains energetics of 1f and reaction enthalpies for all monomers discussed). For the methyl ester monomer (1a), the activation barrier to form the tetrahedral intermediate is 9.1 kcal/mol, which is the highest in the group, but comparable for all the other monomers with phenyl ester leaving groups (Figure 5). The relative position of this transition state (TS#1) represents two factors that are impacting the reaction: (a) the bulkiness of the leaving group and, (b) the relative charge delocalization and stabilization of the transition state (TS#1). Steric effects are evident when considering the reaction of the monomer 1f (see Table S1), where the TS#1 activation barrier is the highest (11.5 kcal/mol) of the groups studied. The bulky tert-butyl moiety prevents the attack of the nucleophile at the carbonyl carbon resulting in a large activation barrier. The second highest activation barrier among the group of compounds considered corresponds to the much less sterically hindered methyl ester monomer 1a.

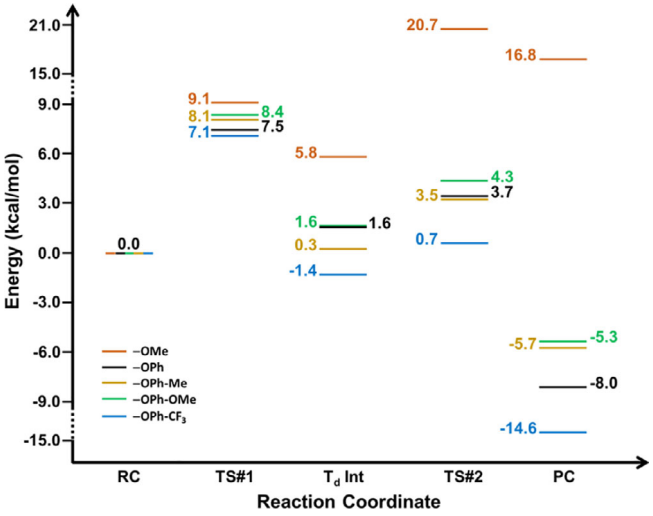

FIGURE 5 Calculated reaction Gibbs free energetics for the polymerization mechanism for 1a (-OMe), 1g (-OPh), 1h (-OPhMe), 1j (-OPhOMe) and 1k (-OPhCF_3) calculated using M06-2X/6–31 + G(d) level of theory. All the numbers shown are in kcal/mol. RC, TS#1, T_d Int, TS#2, and PC correspond to the reactant complex, the transition state for nucleophilic attack to the ester carbonyl carbon, the tetrahedral intermediate, the transition state for the decomposition of tetrahedral intermediate, and the product complex, respectively [Color figure can be viewed at wileyonlinelibrary.com]

Although it may seem that the phenoxide groups are bulkier than the methoxy unit, due to the restrained aromatic ring structure the energy required for the movement of the methoxy group relative to the phenoxide group is perhaps comparable. The difference nonetheless is the relative charge delocalization and stabilization of the transition state (TS#1), which is evident from the charge data shown in Table 5 (vide infra). The negative charge build up on the carbonyl unit is significantly less in case of the monomer 1 k when compared with the rest of the monomers considered and therefore the transition state is more stabilized. This is reflected in the TS#1 activation barriers where the barrier for trifluoromethyl phenyl monomer (1k) is lower when compared with that of any other monomer tested. The barriers slightly increase as a function of increasing electron donating nature of the para substituent on the phenyl unit. It is possible to infer that the electrophilic nature of the ester carbon may play a significant role in the first reaction step. However, it was found not to be the case since the partial atomic charge on the ester carbons for all the monomers considered was almost identical (see Table S2).

The stability of the tetrahedral intermediate is another factor that plays an important role in the rate of CGC polymerization, which involves both the role of steric effects and the delocalization of the negative charge. In the case of the tert-butyl monomer 1f, steric effects again play the major role, resulting in the least stable intermediate. For the phenyl esters, delocalization of the charge appears to be the principal factor. The tetrahedral intermediate is more stable than the reactant complex (RC) only for the trifluoromethyl phenyl substituted monomer (1k). For the rest of the phenyl-based monomers, the tetrahedral intermediate is slightly higher in energy than the RC. Delocalization of the charge into the phenyl ring significantly stabilizes the intermediate when compared with the alkyl monomers 1a and 1f, which lack a phenyl ring and are highly endothermic. As for variation in the phenyl esters, the electron withdrawing nature of the substituent on monomer 1k assists in the delocalization of charge while electron donating groups present on the monomer, such as 1h and 1j, hinder the delocalization causing slightly less stable intermediates (Table 5, vide infra). However, as shown in Figure 5, the tetrahedral intermediate of 1h is strongly stabilized, much more so than 1g and 1j. This observation is attributed to the inadequate estimation of entropic contributions for the calculation of Gibbs free energy. Specifically, for 1h, entropic contributions due to the rotations around C-C bonds are hard to estimate through static minimum energy structure calculations, and therefore it is reflected in the Gibbs free energy of the T_d intermediate. When one looks at the reaction enthalpies (Table S1) instead of Gibbs free energy, this problem is alleviated, and the trend discussed above is maintained.

In the last step of the reaction, the tetrahedral intermediate decomposes via the elimination of the alkoxide anion, which depends primarily upon the stability of the leaving group, that is, the pKa of the alkoxide. In the case of 1f, tert-butoxide is the leaving group which has the highest pKa among the group (Table 2) and, as a result, the calculated energy barrier for the decomposition of the tetrahedral intermediate and the endothermicity of the reaction is also the highest among the groups tested computationally. On the opposite side of the spectrum is 1k, the trifluoromethyl phenyl ester monomer which has the most stable resulting alkoxide as indicated by the pKa of trifluoromethyl phenol, and therefore the decomposition of the intermediate was almost barrierless and the most exothermic among the group. The other alkoxide anions studied follow this pKa trend in decomposition of the tetrahedral intermediate as well.

Upon looking at the overall thermodynamics of the reactions studied, except for monomers 1a and 1f, all the monomer addition reactions are thermodynamically favorable. However, except for the trifluoromethyl phenyl ester monomer 1k, none of the reactions are exothermic until after the decomposition of the tetrahedral intermediate, which primarily depends upon the pKa of the leaving group. The decomposition of the tetrahedral intermediate is the rate limiting step for monomer 1a and 1f, due to the high pKa of the leaving groups, contributing to these reactions being endothermic. As a result, stability of the leaving alkoxide plays a critical role in the CGC mechanism. Even though the overall thermodynamics of the reaction with monomer 1a is unfavorable, it does not mean that the reaction will not take place, though the reaction will slow down significantly at low temperatures. This is consistent with the experiments described above. To analyze the reaction energetics summarized in the Figure 5, partial atomic charges were computed as discussed in the subsequent section.

3.4.2 | Partial atomic charge calculations

As discussed previously, it is well understood that control over CGC polymerizations for the synthesis of aromatic polyamides is established when the reactivity of the deprotonated monomer is higher with the ester on the initiator or polymer end group than the ester on another monomer, resulting in reactions following a chain-growth process. Literature suggests that deactivation of the monomer is achieved by the deprotonation of the aromatic amine on the monomer, thus producing an amide ion that donates charge to the ring and, is thought to,

limit the reactivity of the carbonyl carbon from attack by another deprotonated monomer.[3] To examine this proposed reasoning for obtaining a controlled CGC polymerization process, an NBO analysis was performed to calculate the partial atomic charge on the carbon of the carbonyl group for the various species in the reaction.

The first computational study performed was to support the claim that the electrophilicity of the ester carbonyl carbon is reduced for the deprotonated monomer when compared with the polymer end group. NBO calculations were performed on the system presented in Scheme 4 containing the phenyl R group to predict the inherent electrophilicity by computing the charge on the carbonyl carbon, along with the surrounding oxygen atoms for reference. This experiment was used to compare the relative charges of species present in a typical polymerization and to investigate which species would be the most reactive between the polymer end group (4.1), the deprotonated monomer (4.2), and a polymer end group with one additional monomer (4.3) (see Scheme 4).

The computed charges seen in Table 4 show that the charge on the carbonyl carbon of compound 4.1 is similar to 4.3. This suggests that the "electrophilicity" or positive charge of the carbonyl carbon on the polymer end group remains the same after monomer addition. In addition, calculations show that the deprotonated monomer, 4.2, has a smaller positive charge on the carbon of the ester carbonyl when compared with the polymer end group, due to the donated negative charge from the deprotonated nitrogen. This demonstrates that the reactive monomer does indeed have a less electrophilic carbonyl carbon, suggesting that the reactivity of the ester on the monomer is reduced when compared with the polymer end group. NBO charges are typically independent of basis sets, therefore systematic changes in calculated absolute charges are significant. These results explain why addition of the deactivated monomer preferentially occurs at the growing polymer end group or at an initiator, if any of those species are present and also agrees with the argument put forth by the Yokozawa group, when explaining how to convert step-growth polymerizations to a chain-growth process.[3]

Even though literature focuses principally on the idea that the polymer end group and monomer reactivity is primarily influenced by the relative electrophilicity, or activation/deactivation, of the carbonyl carbon of the ester group, the experimental results previously discussed in this study demonstrate that the reactivity is also greatly affected by the ester substituent. To examine these observations, computational studies were also conducted to examine the effect of the ester substituent on the relative electrophilicity of the various ester carbonyl carbons. As such, the charges on the carbon and oxygen atoms of the ester carbonyl were calculated for the tert-butyl and methyl ester alkyl monomers and the phenyl ester monomers with the various substituents in the para position. These calculations show that variation of the phenyl ester substituent result in very little effect on the electrophilic

TABLE 4 Partial atomic charges computed by NBO analysis using B3LYP/6–31 + G(d) level of theory. Charges computed for atoms surrounding the carbonyl unit participating in the nucleophilic attack for the three carbonyl species depicted in Scheme 4 with a phenyl R group

	Carbonyl investigated		
Atom (in bold)	**4.1**	**4.2**	**4.3**
O═C—**O**R	−0.565	−0.586	−0.563
O═**C**—OR	0.849	0.812	0.850
O═C—OR	−0.624	−0.696	−0.619

TABLE 5 Partial atomic charges computed by NBO analysis using B3LYP/6–31 + G(d) level of theory

Rxn Coord	Atom (bold)	Tert-butyl	Me	Ph	Ph—CH_3	Ph—OCH_3	Ph—CF_3
TS#1	O═C—**O**	−0.643	−0.631	−0.588	−0.589	−0.590	−0.582
	O═**C**—O	0.834	0.816	0.822	0.822	0.820	0.814
	O═C—O	−0.790	−0.795	−0.740	−0.744	−0.750	−0.738
T_dInt	O═C—**O**	−0.683	−0.672	−0.630	−0.630	−0.634	−0.623
	O═**C**—O	0.773	0.759	0.759	0.759	0.759	0.759
	O═C—O	−0.914	−0.914	−0.889	−0.892	−0.894	−0.880
TS#2	O═C—**O**	−0.921	−0.944	−0.742	−0.752	−0.760	−0.701
	O═**C**—O	0.769	0.755	0.759	0.745	0.745	0.759
	O═C—O	−0.717	−0.702	−0.771	−0.773	−0.768	−0.789

Note: Charges computed for atoms surrounding the carbonyl group of the TS#1, T_d Int, and TS#2 complexes formed in the CGC mechanism for each monomer ester substituent under investigation.

nature of the carbonyl carbon (Table S2), despite the large difference in reactivity of these monomers. To gain a better understanding of how the ester substituents effect the activation barriers of the transition states (TS#1 and TS#2) and the stability of the tetrahedral intermediate, partial atomic charges were calculated for the carbonyl group at each position on the reaction coordinate (see Figure 5).

The charges in Table 5 were calculated for the transition state complexes (TS#1 and TS#2) and tetrahedral intermediate formed over the course of the reaction for all the ester R groups studied. These calculations show that variation of the phenyl ester substituent results in changes in charge to the overall carbonyl unit. Charge of the carbonyl carbon for TS#1 varies slightly with change of substituent, however charges on the carbonyl and ester oxygen change significantly with different R groups. Electron donating R groups increase the negative charge on both oxygen atoms while electron withdrawing R groups lower the negative charge resulting in an overall more electrophilic carbonyl unit. The overall electrophilic nature of the carbonyl group impacts the activation barrier for formation of the first transition state as discussed in the previous section. It is evident that upon nucleophilic attack and formation of the tetrahedral intermediate, charge shifts to the carbonyl oxygen (C═O). The amount of charge on the oxygen is dependent on the ester R group. For the alkyl-based monomer, such as the tert-butyl and methyl ester monomers, the charge is the most negative as no charge delocalization is available. However, for the various phenyl ester monomers, charge is less negative on the oxygen atoms due to charge delocalization into the phenyl ring. The trifluoromethyl ester shows the least negative charge (most stable intermediate) as it pulls the increased electron density towards the ring. This result is in accord with observations observed in the enthalpic reaction energetics, the electron withdrawing phenyl esters stabilize the intermediate resulting in lower activation barriers.

Upon decomposition of the tetrahedral intermediate and ejection of the alkoxide anion, the charge shifts from the carbonyl oxygen to the ester oxygen. The amount of charge on the oxygen is again dependent on the R group. The largest negative charges are present on the tert-butyl and methyl ester monomers due to no charge delocalization. The high negative charges are in agreement with large pKa values (Table 2), resulting in the instability of the leaving group. The negative charge of the ester oxygen is significantly different for the phenyl monomers as delocalization of the charge is possible. The charge is the lowest for the trifluoromethyl phenoxide due to the electron withdrawing nature. The charge on the oxygen increases as electron donating strength increases. These observations are in agreement with the reaction energetics presented as the collapse of the tetrahedral intermediate and formation of the anion is primarily dependent on the stability of the leaving group.

While, as discussed in the published CGC mechanism, the electrophilicity of the carbon of the acyl group does indeed play a role in the reactivity of the monomer in the polymerization mechanism, our results demonstrate that in fact, the stability of the first transition state and the leaving group appear to be the main driving forces for the experimental trends observed. The experimental results show that there is a major difference between the kinetics of the methyl ester monomer (1a) when compared with the phenyl ester monomer (1g), despite similar positive charge on the carbonyl carbon for both monomers. This is because the methoxy anion is a relatively unstable leaving group, whereas the phenoxy anion can be stabilized via resonance stabilization. Incorporating an electron donating group in the para position reduces the stabilization of the phenoxy leaving group whereas an electron withdrawing group facilitates the resonance stabilization leading to a more stable phenoxide resulting in a faster overall polymer growth mechanism. These trends are observed in the computed thermodynamics and kinetics of the mechanism and are in agreement with experimental results; see Table 6.

The calculated activation energies are in good agreement with the experimental activation energies in trends alone, and both reveal that the activation energies for the polymer growth mechanism are largely affected by the leaving group substituent group. The tert-butyl ester monomer has the largest barrier to overcome in order for the reaction to proceed with no experimental activation energy obtained, followed by a lower activation energy of

TABLE 6 Activation energies (E_a) calculated by KisThelP software package using B3LYP/6–31 + G(d) level of theory energetics for various alkoxide leaving groups compared with experimentally determined Ea for the CGC polymerization mechanism

Leaving group substituent	Computational E_a (kJ/mol)[a]	Experimental E_a (kJ/mol)[b]
Tert-butyl	64.0	-
Methyl	59.7	51.5
MeO-phenyl	31.6	44.6
H_3C-phenyl	30.4	36.8
Phenyl	29.0	36.2
F_3C-phenyl	24.3	34.9

[a]Corresponds to the rate limiting step.
[b]Error is ±0.1 kJ/mol.

the more successful methyl ester monomer. We believe that steric effects, poor stability of the tetrahedral intermediate, and high pKa of the leaving group contributes to the large computed activation energy and the experimental observation of no reaction occurring for the tert-butyl group, and only the basicity of the less hindered methoxide anion contributes to the low but successful reactivity of the ester. The lower energy barriers attributed to the phenyl ester monomers correspond to the lower basicity and higher anion stabilization, especially with the electron withdrawing trifluoromethyl group and facilitate the phenoxide ejection portion of the mechanism. The electron withdrawing group helps to pull charge into the ring, stabilizing the negative charge of the leaving group. However, electron donating groups push the charge onto the oxygen making it harder to separate after attack from the amide nucleophile.

4 | CONCLUSIONS

In attempt to improve upon the well-studied literature surrounding the polymerization of the methyl ester aminobenzoate monomers in CGC polymerizations, studies were performed to investigate the potential use of monomers with varying ester substituents. Monomers with varying ester groups ranging from n-alkyl and branched esters to substituted phenyl esters were synthesized and polymerized to study the solubility and polymerization effectiveness. Monomer ester substituents were chosen as candidates by examining the solubility of the produced lithium alkoxides over the methyl analogue. Even though the branched alkyl esters, (containing the isopropyl and tert-butyl group) produced very soluble alkoxides in THF solution, they were very poor at producing polymers at high conversion and kinetic studies demonstrated that they remained relatively unreactive. This was believed to be due to their high pKa's and steric blocking of the ester carbonyl carbon. The phenyl ester derivative monomers all showed impressive solubility when in the lithium phenoxide form and produced crystal clear solutions post polymerization. Kinetic studies showed that the phenyl ester monomers had k_p values one to three orders of magnitude higher than the methyl ester monomer. The order in phenyl ester monomer reactivity followed the pKa values of the conjugate acids for the lithium phenoxides produced as a byproduct of the reaction. The obtained experimental results were supported by computational studies, which demonstrated that the stability of the alkoxide or phenoxide was the major contributor to the reactivity of the monomers and a dominant factor in the overall CGC polymerization mechanism. The reaction energetics for the nucleophilic acyl substitution reaction demonstrate that while the reactivity of the carbonyl carbon plays an important role in the first step of the reaction, dissociation of the tetrahedral intermediate to form the substitution product, the step that dominates the overall thermodynamics of the reaction, is dominated by the basicity of the leaving group. These results provide greater insight to the CGC polymerization mechanism and highlight the important of factors not previously considered in the published mechanism.

ACKNOWLEDGMENTS

S. G. B. gratefully acknowledges the support of this work by the National Science Foundation under grant CHE MSN #1807863. B. D. E. and S. V. gratefully acknowledge the computational resources from high performance computing facility at CSM.

ORCID

Stephen G. Boyes https://orcid.org/0000-0003-4821-2785

REFERENCES

[1] A. Rudin, P. Choi, *The Elements of Polymer Science & Engineering*. Elsevier, Waltham, MA **2013**, p. 305.
[2] T. Yokozawa, A. Yokoyama, *Chem. Rev.* **2009**, *109*, 5595.
[3] T. Yokozawa, A. Yokoyama, *Chem. Rec.* **2005**, *5*, 47.
[4] A. Kiriy, V. Senkovskyy, M. Sommer, *Macromol. Rapid Commun.* **2011**, *32*, 1503.
[5] Z. J. Bryan, A. J. McNeil, *Macromolecules* **2013**, *46*, 8395.
[6] T. Yokozawa, Y. Ohta, *Chem. Rev.* **2016**, *116*, 1950.
[7] A. Yokoyama, T. Yokozawa, *Macromolecules* **2007**, *40*, 4093.
[8] T. Yokozawa, A. Yokoyama, *Prog. Polym. Sci.* **2007**, *32*, 147.
[9] T. Yokozawa, Y. Ohta, *Chem. Commun.* **2013**, *49*, 8281.
[10] T. Yokozawa, M. Ogawa, A. Sekino, R. Sugi, A. Yokoyama, *Macromol. Symp.* **2003**, *199*, 187.
[11] F. C. Prehn, S. G. Boyes, *Macromolecules* **2015**, *48*, 4269.
[12] J. M. García, F. C. García, F. Serna, J. L. de la Peña, *Prog. Polym. Sci.* **2010**, *35*, 623.
[13] T. Yokozawa, T. Asai, R. Sugi, S. Ishigooka, S. Hiraoka, *J. Am. Chem. Soc.* **2000**, *122*, 8313.
[14] T. Yokozawa, D. Muroya, R. Sugi, A. Yokoyama, *Macromol. Rapid Commun.* **2005**, *26*, 979.
[15] R. Sugi, A. Yokoyama, T. Furuyama, M. Uchiyama, T. Yokozawa, *J. Am. Chem. Soc.* **2005**, *127*, 10172.
[16] R. Sugi, T. Ohishi, A. Yokoyama, T. Yokozawa, *Macromol. Rapid Commun.* **2006**, *27*, 716.
[17] Y. Ohta, S. Fujii, A. Yokoyama, T. Furuyama, M. Uchiyama, T. Yokozawa, *Angew. Chem. Int. Ed.* **2009**, *48*, 5942.
[18] M. J. Frisch, G. W. Trucks, H. B. Schlegel, G. E. Scuseria, M. A. Robb, J. R. Cheeseman, G. Scalmani, V. Barone, B. Mennucci, G. A. Petersson, H. Nakatsuji, M. Caricato, X. Li, H. P. Hratchian, A. F. Izmaylov, J. Bloino, G. Zheng, J. L. Sonnenberg, M. Hada, M. Ehara, K. Toyota, R. Fukuda, J. Hasegawa, M. Ishida, T. Nakajima, Y. Honda, O. Kitao, H. Nakai, T. Vreven, J. A. Montgomery Jr., J. E. P, F. Ogliaro, M. Bearpark, J. J. Heyd, E. Brothers, K. N. Kudin, V. N.

Staroverov, R. Kobayashi, J. Normand, K. Raghavachari, A. Rendell, J. C. Burant, S. S. Iyengar, J. Tomasi, M. Cossi, N. Rega, J. M. Millam, M. Klene, J. E. Knox, J. B. Cross, V. Bakken, C. Adamo, J. Jaramillo, R. Gomperts, R. E. Stratmann, O. Yazyev, A. J. Austin, R. Cammi, C. Pomelli, J. W. Ochterski, R. L. Martin, K. Morokuma, V. G. Zakrzewski, G. A. Voth, P. Salvador, J. J. Dannenberg, S. Dapprich, A. D. Daniels, Ö. Farkas, J. B. Foresman, J. V. Ortiz, J. Cioslowski, D. J. Fox, *Gaussian, Inc.*, Wallingford CT **2016**.

[19] Y. Zhao, D. G. Truhlar, *Theor. Chem. Accounts* **2008**, *120*, 215.

[20] W. J. Hehre, K. Ditchfield, J. A. Pople, *J. Chem. Phys.* **1972**, *56*, 2257.

[21] P. C. Hariharan, J. A. Pople, *Theor. Chim. Acta* **1973**, *28*, 213.

[22] V. Barone, M. Cossi, J. Tomasi, *J. Comput. Chem.* **1998**, *19*, 404.

[23] J. P. Foster, F. Weinhold, *J. Am. Chem. Soc.* **1980**, *102*, 7211.

[24] S. Canneaux, F. Bohr, E. Henon, *J. Comput. Chem.* **2014**, *35*, 82.

[25] Y. Ohta, T. Shirakura, A. Yokoyama, T. Yokozawa, *J. Polym. Sci. Part A Polym. Chem.* **2013**, *51*, 1887.

[26] T. Ohishi, R. Sugi, A. Yokoyama, T. Yokozawa, *J. Polym. Sci. Part A Polym. Chem.* **2006**, *44*, 4990.

[27] T. Ohishi, R. Sugi, A. Yokoyama, T. Yokozawa, *Macromolecules* **2008**, *41*, 9683.

[28] K. Yoshino, A. Yokoyama, T. Yokozawa, *J. Polym. Sci. Part A Polym. Chem.* **2009**, *47*, 6328.

[29] K. Yoshino, K. Hachiman, A. Yokoyama, T. Yokozawa, *J. Polym. Sci. Part A Polym. Chem.* **2010**, *48*, 1357.

[30] Y. Ohta, Y. Kamijyo, A. Yokoyama, T. Yokozawa, *Polymers (Basel).* **2012**, *4*, 1170.

[31] R. Sugi, D. Tate, T. Yokozawa, *J. Polym. Sci. Part A Polym. Chem.* **2013**, *51*, 2725.

[32] K. Iwashita, H. Katoh, Y. Ohta, T. Yokozawa, *Polymers (Basel)* **2017**, *9*, 246.

[33] C. W. Kamienski, D. H. Lewis, *J. Org. Chem.* **1965**, *30*, 3498.

[34] E. M. Arnett, K. D. Moe, *J. Am. Chem. Soc.* **1991**, *113*, 7288.

[35] D. D. Perrin, *Pure Appl. Chem.* **1969**, *20*, 133.

[36] T. Yokozawa, M. Ogawa, A. Sekino, R. Sugi, A. Yokoyama, *J. Am. Chem. Soc.* **2002**, *124*, 15158.

[37] Y. Ohta, M. Karasawa, T. Niiyama, A. Yokoyama, T. Yokozawa, *J. Polym. Sci. Part A Polym. Chem.* **2014**, *52*, 360.

[38] Y. Ohta, T. Niiyama, A. Yokoyama, T. Yokozawa, *J. Polym. Sci. Part A Polym. Chem.* **2014**, *52*, 1730.

[39] K. Yoshino, A. Yokoyama, T. Yokozawa, *J. Polym. Sci. Part A Polym. Chem.* **2011**, *49*, 986.

[40] C. G. Mitton, M. Gresser, R. L. Schowen, *J. Am. Chem. Soc.* **1969**, *91*, 2045.

[41] F. M. Menger, J. H. Smith, *J. Am. Chem. Soc.* **1972**, *94*, 3824.

[42] H. Zipse, L.-H. Wang, K. N. Houk, *Liebigs Ann.* **1996**, *1996*, 1511.

[43] L.-H. Wang, H. Zipse, *Liebigs Ann.* **1996**, *1996*, 1501.

SUPPORTING INFORMATION

Additional supporting information may be found online in the Supporting Information section at the end of this article.

How to cite this article: Prehn FC Jr, Etz BD, Reese CJ, Vyas S, Boyes SG. Chain-growth polycondensation via the substituent effect: Investigation of the monomer structure on synthesis of poly(N-octyl-benzamide). *J Polym Sci*. 2020;58:2389–2406. https://doi.org/10.1002/pol.20200435